Food Hydrocolloids 23 (2009) 577–584

Contents lists available at ScienceDirect

Food Hydrocolloids

journal homepage: www.elsevier.com/locate/foodhyd

Effects of concentration on nanostructural images and physical properties of gelatin from channel catfish skins

Hongshun Yang [a,b], Yifen Wang [a,*]

[a] Biosystems Engineering Department, Auburn University, 200 Tom E. Corley Building, Auburn, AL 36849-5417, USA
[b] College of Food Science and Technology, Henan University of Technology, Zhengzhou, Henan 450052, PR China

ARTICLE INFO

Article history:
Received 25 January 2008
Accepted 17 April 2008

Keywords:
Nanostructure
Atomic force microscopy (AFM)
Viscosity
Gel strength
Gelatin
Nanotechnology
Fish skin

ABSTRACT

Physical properties are crucial to gelatin utilization and the physical properties are determined by structure. Therefore, it is important to investigate the nanostructure and physical properties of gelatin over the full range of concentrations which are widely applied in research and industry. Nanostructure of gelatin can be investigated by atomic force microscopy (AFM). However, it is hard to obtain reliable AFM images of gelatin with high concentrations (1–6.67%). In this study, methods for imaging gelatin with high concentration were explored and developed, which mainly included six steps. Then the relationships among concentration, nanostructure and physical property of gelatin extracted from channel catfish skins (*Ictalurus punctatus*) were studied. The high-resolution AFM images show fibril structure in gelatins with concentrations from 1% to 6.67%. However, in low concentrations (<1%), most nanostructures of gelatin were spherical aggregates and fibril structure only existed occasionally. Correspondingly, there were no significant differences of gel strength, texture profile and viscosity among several groups of gelatin when the concentration was lower than 1%, in contrast, these properties changed dramatically when the concentration was greater than 1%. It indicates that there must be some close relationships among concentration, nanostructure and physical property of gelatin. The illustration of nanoscale transition would help us understand the macroscale changes of physical properties.

1. Introduction

Gelatin is the hydrolyzed product of collagen and has been widely used in food, pharmaceutical, and photographic industries. Currently, most of the gelatin is obtained from the hide and bone of mammals. However, fish skins are alternative materials for gelatin production because of safety, economic, religious, and environmental considerations (Yang, Wang, Jiang, et al., 2007). Physical properties are crucial to gelatin utilization and because the physical properties of gelatin are determined by its structure, including the protein sequence, relative contents of components, and their aggregations, it is important to investigate the structure of fish skin gelatin before application.

Previously, the structures of gelatin were studied by GC/HPLC (Jamilah & Harvinder, 2002), rheometer (Jamilah & Harvinder, 2002), spectrometer (Nordmark & Ziegler, 2000), SEM/TEM (Djabourov et al., 1993; Saxena, Sachin, Bohidar, & Verma, 2005), electrophoretic analysis (Gómez-Guillén et al., 2002; Zhou, Mulvaney, & Regenstein, 2006), differential scanning calorimetry (Badii & Howell, 2006), and FT-IR spectroscopy (Badii & Howell, 2006). However, high heterogeneity of gelatin structure prevents further illustration of the detailed information. Except for SEM/TEM, most of the above-techniques give sample-wide average information. For SEM/TEM, the complicated pretreatment of samples sometimes obscures the sample's native structure, and sometimes, samples deviate from their native status after preparation (Yang, Wang, Lai, et al., 2007).

Nanotechnology is promising in studying structure at the nanoscale level in food science, including food protein gels (Foegeding, 2006; Yang, Wang, Lai, et al., 2007). Atomic force microscopy (AFM), as one of the nanotechnology tools, has been successfully applied to the study of food polysaccharides (An, Yang, Liu, & Zhang, 2008; Yang, Lai, An, & Li, 2006), gelatin from high-purity laboratory-prepared mammalian samples (Benmouna & Johannsmann, 2004; Chen et al., 1998; Haugstad & Gladfelter, 1993, 1994; Lin et al., 2002; Mackie, Gunning, Ridout, & Morris, 1998; Mohanty & Bohidar, 2005; Radmacher, Fritz, & Hansma, 1995; Saxena et al., 2005; Uricanu, Duits, Nelissen, Bennink, & Mellema, 2003; Yao, Liu, Lin, & Qiu, 1999), and recently gelatin from fish skins (Wang, Yang, & Regenstein, 2008; Yang, Wang, Regenstein, & Rouse, 2007; Yang, Wang, Zhou, & Regenstein, 2008). However, it is still difficult to correlate the nanostructural information obtained from

* Corresponding author. Tel.: +1 334 844 8051; fax: +1 334 844 3530.
E-mail address: wangyif@auburn.edu (Y. Wang).

0268-005X/$ – see front matter © 2008 Elsevier Ltd. All rights reserved.
doi:10.1016/j.foodhyd.2008.04.016

AFM with physical properties due to the restriction of imaging conditions. With regular sample preparation for AFM imaging, gelatins should be diluted to a very low concentration before imaging, which is far from the concentration of practical application (Haugstad & Gladfelter, 1993, 1994; Lin et al., 2002; Mackie et al., 1998; Radmacher et al., 1995; Yao et al., 1999). To our best knowledge, no delicate structural information of high concentration gelatin has been reported. So far, gelatin is not as well defined structurally as other synthetic polymers (Benmouna & Johannsmann, 2004).

The objectives of this work were to develop the sample preparing methods to enable AFM image fish gelatin with high concentration directly without dilution and to establish some relationships between the nanostructure and physical property of gelatin with different concentration. To fulfill the objectives, sample preparing methods were explored and improved for high concentration gelatins to obtain delicate structural information at a nanoscale level. AFM images of different concentration gelatins were obtained and were correlated with the results of texture and viscosity determination. The concentrations used here were in the range of research and industry related application.

2. Materials and methods

2.1. Preparation of different concentrations of gelatin

A previously developed procedure of gelatin extraction was used for gelatin preparation (Yang, Wang, Jiang, et al., 2007). All reagents used in this study were analytical grade. Frozen catfish skins (Harvest Select Inc., Uniontown, AL, USA) were stored at −18 °C with a maximum storage time of less than 2 months before use. The frozen skins were thawed at 4 °C for about 20 h, then cut into small pieces (about 2–3 cm squares) and washed with tap water (1:6 w/v) at 4 °C for 10 min. Washing was repeated two more times. The cleaned fish skins were drained using four layers of cheesecloth for 5 min, and the cheesecloth containing the skins was then squeezed by hand to remove the liquid as much as possible. Cleaned skins were put into a flask and treated with 0.20 M NaOH (1:6 w/v) for 84 min. Then, the samples were drained, including the hand-squeezing step using the cheesecloth, and rinsed with tap water (1:6 w/v). The above procedure was repeated two times, and then the samples were treated with 0.115 M acetic acid (1:6 w/v) for 60 min, drained using the cheesecloth and rinsed with tap water (1:6 w/v) three times. All of the solutions used in the above steps were kept at 4 °C. After the above pretreatment, deionized water (1:4 w/v) was added to the flasks. Parafilm and aluminum foil were then used to cover the flasks and samples were kept in a 55 °C water bath (Model 86; Precision Scientific Co., Chicago, IL, USA) for 180 min. After that, the gelatin solutions were filtered through four layers of cheesecloth, and then the solution was lyophilized (Labconco Corporation, Kansas City, MO, USA). When we conducted the AFM experiment of gelatin, the lyophilized gelatin was dissolved to 6.67% (w/w) in distilled water, a standard concentration at which physical properties are determined (Wainewright, 1977). The mixture was allowed to stand until the gelatin was completely swollen. Then it was heated and stirred at 65 °C by a magnetic stirrer (Model 310T, Fisher Scientific Inc., Pittsburgh, PA, USA) until the gelatin was fully dissolved (approximately 30 min). Finally, the solution was diluted to 3.3%, 1%, 0.5%, 0.25%, 0.1% and 0.05%, respectively.

Part of each diluted solution was taken out for AFM characterization and viscosity determination. The remaining part of each solution was then put into small cylindrical-shaped plastic bottle (Wheaton Industries Inc., Millville, NJ, USA), that has flat bottom, with upper part internal dia of 33 mm, lower part dia of 29 mm and height of 25 mm. After cooling down to the room temperature it was kept in a refrigerator at 10 °C for 17 ± 1 h.

2.2. Determination of physical properties of gelatin

2.2.1. Determination of gel strength and texture profile analysis

After being matured at 10 °C for 17 ± 1 h, the gel was removed from the bottle using a thin blade knife. In each lot, some gels were used for gel strength and remains for texture profile analysis (TPA). The TA.XTPlus Texture Analyzer (Texture Technologies Corp., Scarsdale, NY/Stable Micro Systems, Godalming, Surrey, UK) was used for determining gel strength with a 12.5-mm-diameter flat plastic plunger pressing 4 mm into the gelatin gel at a speed of 1 mm/s. The sample was assumed to have a temperature of 10 °C since it was measured immediately after being removed from 10 °C refrigeration (Wainewright, 1977).

TPA was performed with the TA.XTPlus Texture Analyzer using a 75-mm-diameter plate with a 40% compression. The detailed test settings were: pre-test speed: 1.0 mm/s; test speed: 0.5 mm/s; post-test speed: 0.5 mm/s; target mode: distance; distance of compression: 10.000 mm (the height of the gel is 25 mm); time: 10.0 s; trigger type: auto (force); trigger force: 0.05 N; tare mode: auto; and advanced options: on.

Textural parameters including hardness, cohesiveness, springiness and chewiness were calculated from the TPA curve as shown in Yang, Wang, Jiang, et al. (2007).

2.2.2. Determination of viscosity

Viscosity (V, cP) of different concentration gelatins was determined using a Cannon–Fenske routine viscometer (Cannon Instrument Co., State College, PA, USA) in a 60 °C water bath (Yang, Wang, Jiang, et al., 2007). The efflux time was recorded using a stopwatch. The densities of the gelatins were determined by weight/volume. The viscosity can then be calculated from the equation: viscosity (cP) = efflux time (s) × viscometer constant (cSt/s) × density of the measured solution (g/mL).

2.3. AFM imaging

The different concentration gelatins were equilibrated to room temperature and then heated in a hot water bath (60 °C) until fully melted. After that, the melted solutions were disrupted to disaggregate any remaining gels to create a homogeneous mixture using a Vortex mixer (Fisher Scientific, Pittsburgh, PA, USA). A small volume (about 20 μl) of the solution was pipetted rapidly (taking about 5 s) onto a piece of freshly cleaved mica sheets (about 1.0 × 1.0 cm^2) (Muscovite Mica, Electron Microscopy Sciences, Hatfield, PA, USA). The solution on the mica surface was then dried using a pipette bulb to make it evenly distributed. The mica with the sample was attached to a 15-mm-diameter AFM specimen disc (TED Pella Inc., Redding, CA, USA) using double-sided adhesive tapes. The disc was then magnetically mounted onto the sample stage.

An AFM (Nano-R2™, Pacific Nanotechnology, Inc., Santa Clara, CA, USA) was applied to characterize the nanostructure in air at ambient temperature using noncontact mode. A Z scanner was applied and detailed information is available in a previous report (Yang, Wang, Regenstein, & Rouse, 2007). The noncontact mode in this AFM is similar to the commonly mentioned tapping mode found in other AFM equipments. The NSC 11/no Al (MikroMasch, Wilsonville, OR, USA) tip (resonance frequency: 330 KHz; force constant: 48 N/m) was used. Scan speed was about 0.2–1 Hz.

2.4. AFM image analysis

The AFM images were analyzed offline with software (Nano-Rule+™ 2.0 user's manual, 2004). Electronic noise was reduced in the raw data by leveling to improve the image quality. The bright and dark areas in the images corresponded to peaks and troughs,

respectively, of the gelatin molecules or aggregates on the mica surface. The height mode and the error-signal mode (both include plane and 3D) were used to display the results. The dimensions (diameter, length, width and height) of the observed aggregates were measured by section analysis, which was done using the AFM software (Yang, Wang, Lai, et al., 2007; Yang, Wang, Regenstein, & Rouse, 2007).

2.5. Statistical analysis

All of the textural analyses and viscosity determinations were conducted in triplicate and the data were reported as a format of mean ± standard deviation. Dozens of parallel imaging tests for gelatin of each concentration were conducted by AFM to obtain reliable, representative and statistically valid results. ANOVA ($P < 0.05$) and Duncan's multiple range test were applied to determine differences among different groups using SAS (Version 9.1.3, Statistical Analysis Systems, Cary, NC, USA). Comparisons that yielded P values <0.05 were considered significant.

3. Results and discussion

3.1. Exploration and development of the sample preparing methods for AFM imaging high concentration gelatin

Researchers have tried several ways to capture images of the gelatins with high concentration. In terms of image mode, tapping mode can largely reduce the amount of lateral forces usually present in the conventional contact mode and it is not sensitive to drift of the cantilever (Radmacher et al., 1995). However, a strong adhesive force will prohibit obtaining the genuine topographical information (Uricanu et al., 2003). Imaging in liquid (butanol and propanol, for instance) is one approach for decreasing the adhesive force between the tip and the sample and also helps to increase the resolution, consequently, decreasing the damage of both the tip and the sample (Mackie et al., 1998; Yang, Wang, Lai, et al., 2007). However, it was found that some scan lines in the center portion of the image are missing due to drift in the system and lift off of the tip off the sample when the image is captured in liquid (Radmacher et al., 1995), furthermore, the liquid may alter the structure of the imaged materials, including gelatin (Yang, Wang, Lai, et al., 2007).

Haugstad and Gladfelter (1994) obtained relatively high resolution images by applying a large negative load (~20 nN) to minimize the contact force between the tip and the sample and employing an offline Fourier filtering to remove most of the small-wavelength noise. However, the large negative load accompanied by a greater propensity for sample disruption and the tips broke off (resulting from a sudden return to the characteristic, rate-independent adhesive force to the tip) or became blunt (reflected in a rate-dependent adhesive force much greater), and would result in a worse imaging resolution. The offline filtering could not improve the resolution of imaging and definitely changed the original structure for improving the resolution.

In general, it is hard or impossible to capture an image on soft gelatin samples without any damage according to the previous report (Radmacher et al., 1995). Direct imaging often obscures the molecular structure for soft gels. It is found that the tip–sample interaction has a strong impact on the images obtained. The tip might pull the gel during imaging. Therefore, the strong adhesion will result in distorted topographical images (Uricanu et al., 2003). Furthermore, gelatin films were susceptible to penetration by the AFM tip (Haugstad & Gladfelter, 1994). It was assumed that the best resolution can be achieved only on hard samples (Radmacher et al., 1995). In conclusion, even though a blunt cone tip terminated by a round apex was used, AFM imaging is still prone to give artifacts for imaging gelatin with all modes (Uricanu et al., 2003). Consequently, the images obtained cannot be viewed as genuine gelatin structure since the contaminated tip would influence the next image (Yang, An, Feng, & Li, 2005). Similar phenomena happened in our experiments on gelatins with high concentrations (6.67% and 3.33%) if using the previous sample preparing methods as applied to low concentration gelatins (Yang, Wang, Regenstein, & Rouse, 2007). Tall parts (Fig. 1a–d) contaminated the tip and resulted in unreal structural information, even though a relatively a small smooth surface can be imaged successfully (Fig. 1e–h).

Based on experience and knowledge mentioned above, several steps were explored and developed in our study to obtain high quality AFM images of gelatin. First, the mica was tilted for about 30–45° before the gelatin solution was pipetted onto it, which facilitated the mobility of the solution and accelerated the drying speed. Second, a pipette bulb was used instead of letting the sample dry naturally in air. Forced air generated by the pipette bulb could extend the solution to a larger area than static ambient does. Third, a higher temperature water bath was used for melting the solution before imaging, which also increased the mobility of the solution. For instance, heating at 60 °C was much better than 40 °C for imaging of gelatin with high concentration. Fourth, decreasing the volume of pipetted gelatin solution lowered the height of the sample and resulted in a relative smooth surface (from 20 μl to 10 μl, for instance). Fifth, blew a relative large volume of the solution on the mica using a pipette bulb and then wiped out the border of the samples, leaving the central part for imaging. Finally, the exposing time before imaging was increased from 30 min to more than 24 h in a small box (to prevent sample from possible pollutants in the surrounding ambient air) (Radmacher et al., 1995), which greatly decreased the adhesive force between the tip and the sample. With the above steps, a very sharp tip was applied for imaging, which greatly improved the resolution of images, and the tip was not trapped in the gel. Among these steps, the second and the final steps were critical. With these steps, high resolution AFM images were successfully obtained on gelatins with high concentration for a small area (<20 μm × 20 μm) (Fig. 2a–d) as well as a large one (50 μm × 50 μm) (Fig. 2e–h). Increasing the exposing time of the sample in air before scanning the sample resulted in a rather smooth surface for imaging (Fig. 3e–h). Some figures were in error-signal mode for showing better features (Fig. 1g, h; Fig. 2c, d, g, h; Fig. 3c, d, f). In error-signal mode, the AFM is operated in constant height. Slow variations in topography are removed and the edges of samples in the images are highlighted. This mode images are particularly useful for imaging very flat samples at high resolution (Yang, Wang, Lai, et al., 2007). This may result from the alignment of macromolecules and evaporation of water with time, which greatly decreases the adhesive force between the tip and the sample.

We noticed that the surface of gel was dehydrated in some degree but the inner part of gel under surface should hold most of the moisture content. In addition, the high concentration gelatin itself had strong water holding capability. The dehydrated surface might deviate a little bit from "true" status. However, it was the maximum natural status could be imaged.

3.2. Effect of concentration on nanostructures and physical properties of gelatin

Our results show that high concentration gelatin (from 1% to 6.67%) had fibril structure (Figs. 2 and 3 show the gelatins with 6.67% and 3.33%, respectively), however, for the low concentration gelatin, most of the structural morphology was spherical aggregates (as shown in Fig. 4), only occasional fibril structure could be observed (Fig. 4e, f). Larger fibrous structures appearing with increasing concentration indicated that they might be bundles of triple helices. As the concentration increased, the number of fibers

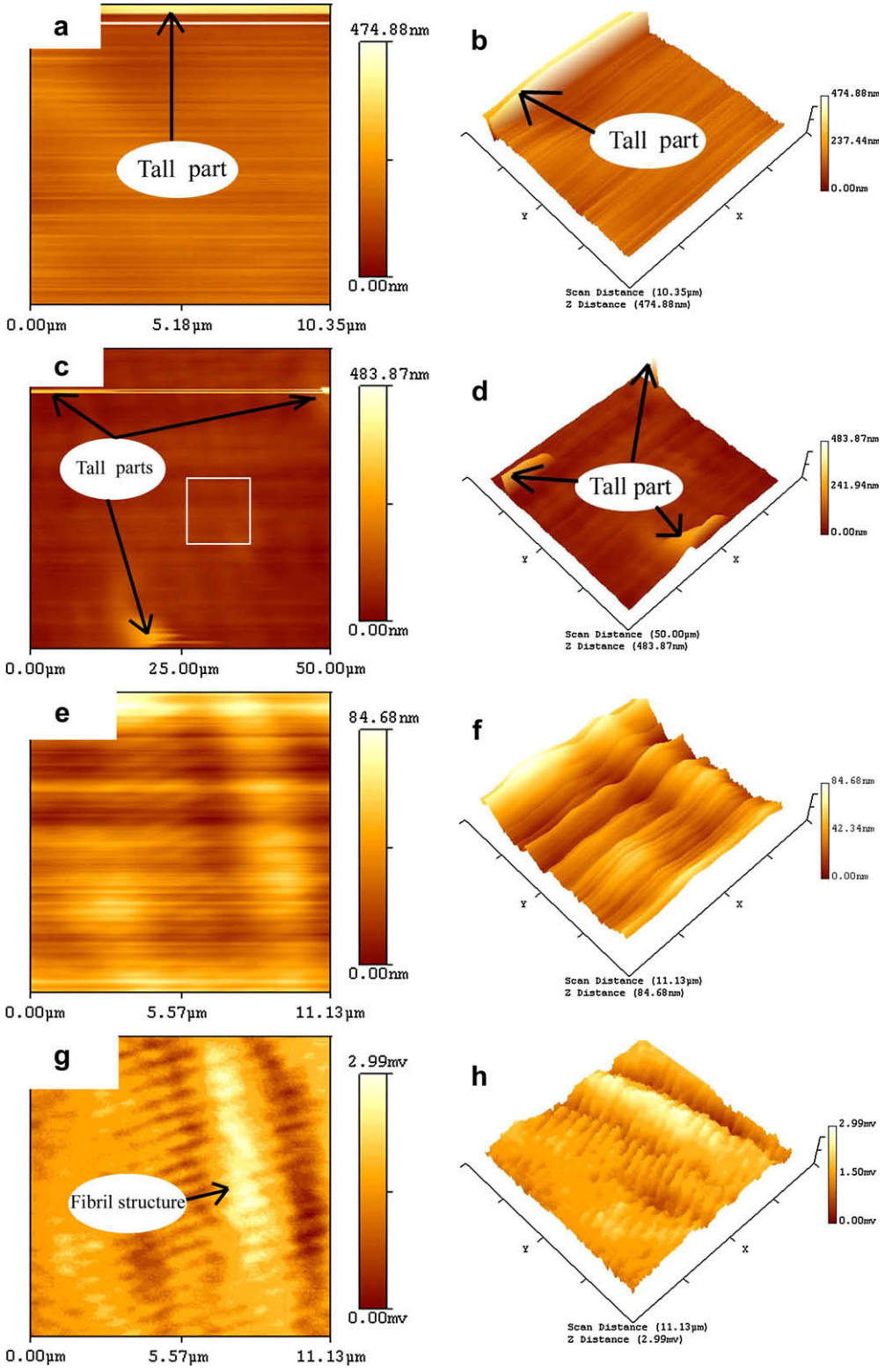

Fig. 1. AFM images of high concentration gelatin without improving sample preparing methods. (a) Plane image of 3.33% gelatin and (b) corresponding 3D image; (c) plane image of 6.67% gelatin and (d) corresponding 3D image; (e) enlarged plane image of c and (f) corresponding 3D image; (g) corresponding error-signal mode image and (h) corresponding 3D image.

increased probably at the expense of spherical aggregates, eventually assembling into a fibrous network, which was similar to the process of gelation with time (Mackie et al., 1998). The morphological assessment of the spherical aggregates and fibril structures was consistent with the observation by Saxena et al. (2005).

From the collagen structural information that has been reported, collagen fibers comprised of tropocollagen are assembled in a specific way giving the collagen a repeat distance of 67 nm. The native tropocollagen molecules are right-handed triple helices with a length of 300 nm and diameter of about 1.5 nm (Mackie

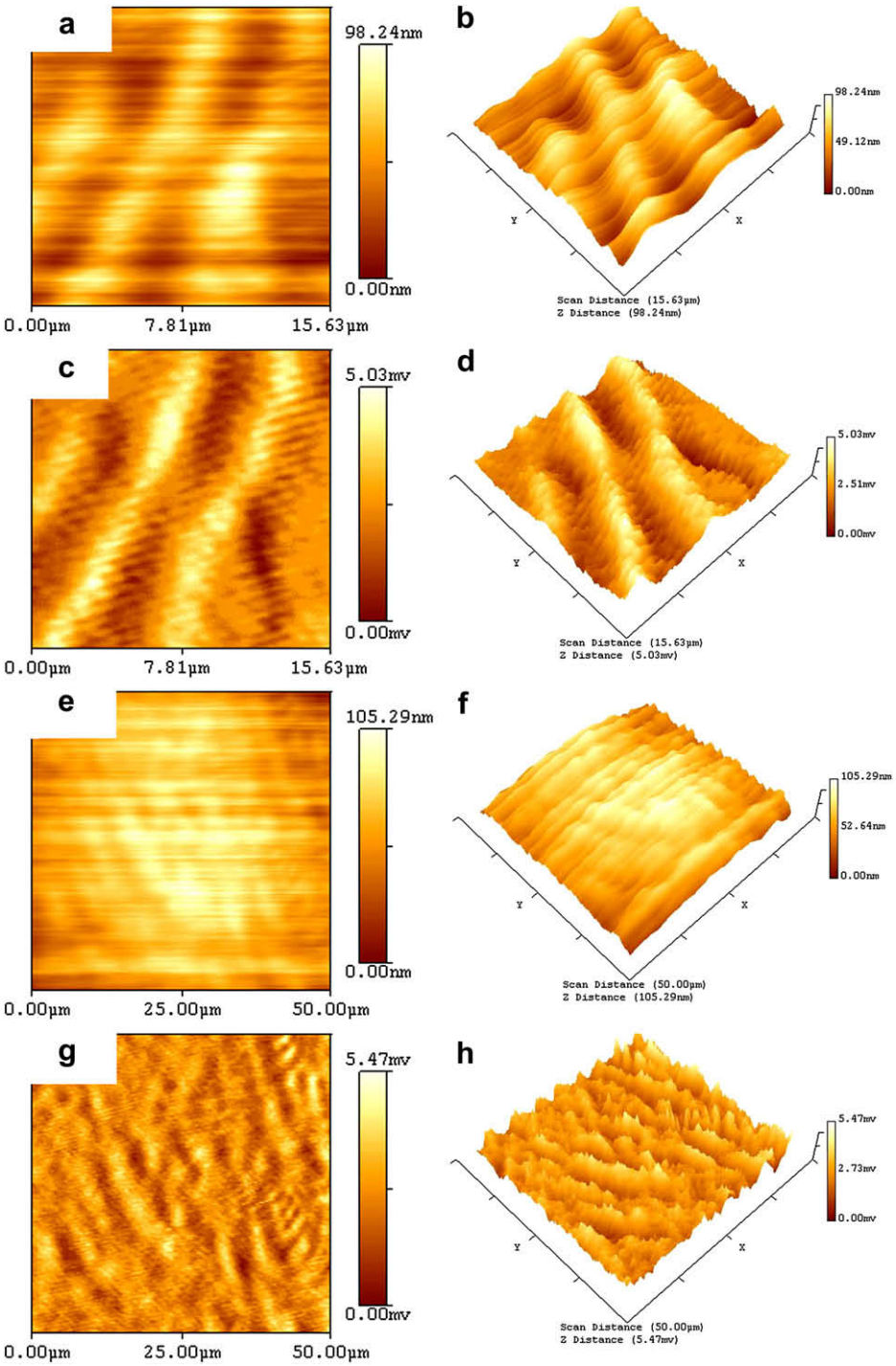

Fig. 2. AFM images of high concentration gelatin with developed sample preparing methods. (a) Plane image of a small area and (b) corresponding 3D image; (c) corresponding error-signal mode image of a and (d) corresponding 3D image; (e) plane image of a large area and (f) corresponding 3D image; (g) corresponding error-signal mode image of e and (h) corresponding 3D image. Note: the concentration of gelatin is 6.67%.

et al., 1998). For gelatin with a high concentration, the width of main-chains was about 2–4 μm (Fig. 3g), which suggests that gelatin was aggregated from newly formed triple helices from denatured collagen and some amount of remaining water.

Until now, little has been known about the structure of gelatin coacervates (Mohanty & Bohidar, 2005). The AFM images show lumps of dense matter with immense heterogeneity spread in space having no definite geometric structures (Mohanty & Bohidar, 2005). However, concentration is believed to be one of the factors that determine the form of the network. At certain concentrations, a gelatin gel is believed to contain junction zones produced by intermolecular triple helix formation (Mackie et al., 1998). Formation of triple helices in the polymer matrix is a major part of the gelation process (Radmacher et al., 1995), which was similar to the transition from small spherical aggregates to a large fibril structure in our results (Fig. 4e, f). Spherical particles only existed in the groups with concentrations not greater than 1%. These spherical particles were similar to the diluted solution of gelatin that was

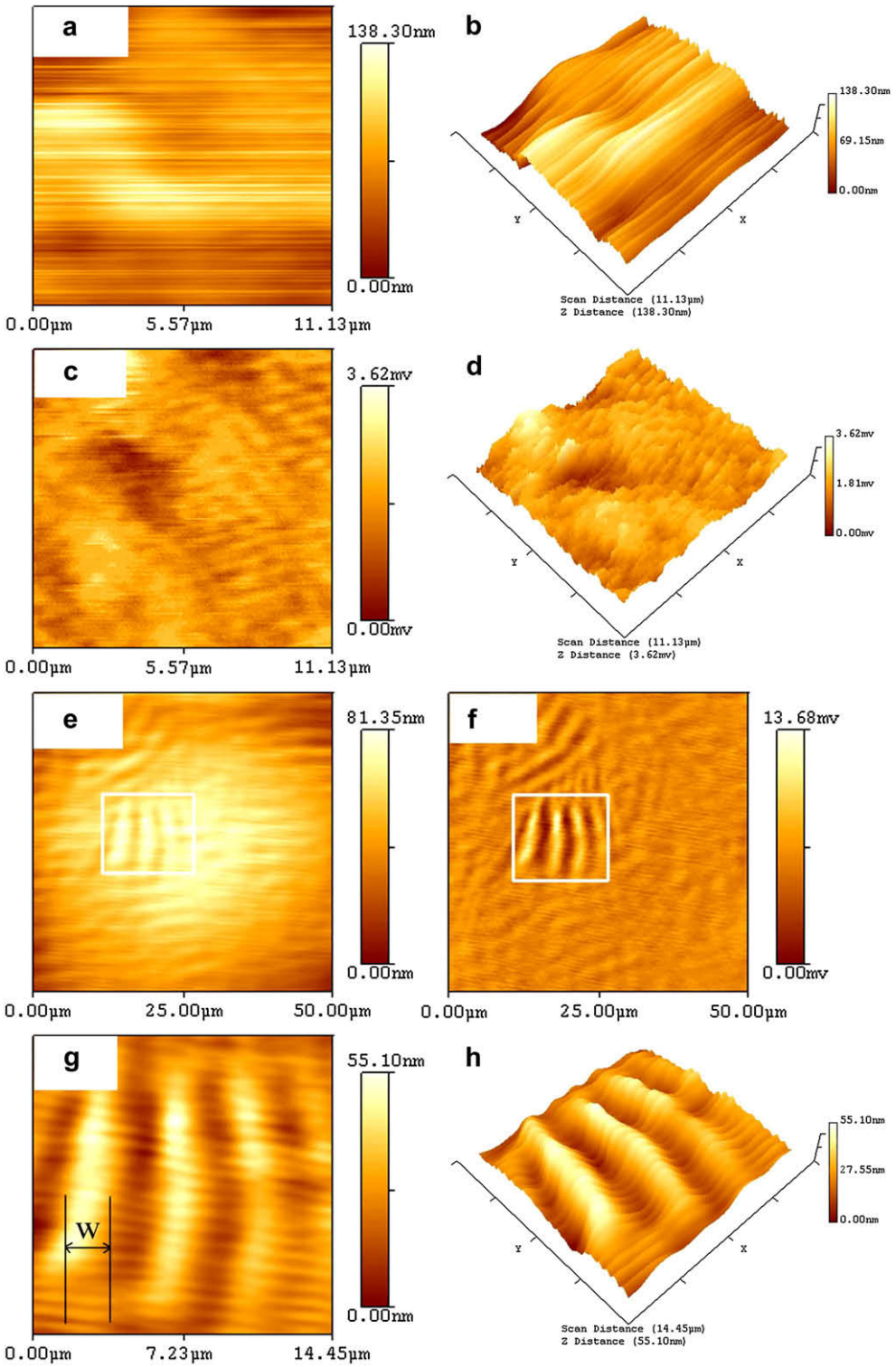

Fig. 3. Effect of storage time on the AFM imaging of high concentration gelatin. (a) Plane image and (b) corresponding 3D image; (c) corresponding error-signal mode image of a and (d) corresponding 3D image; (e) plane image and (f) corresponding error-mode image; (g) enlarged plane image of e and (h) corresponding 3D image. Note: a, b, c, d: imaged after prepared for 1 day; e, f, g, h: imaged after prepared for 8 days. The concentration of gelatin is 3.33%. W: width of fibril structure of gelatin.

reported (Uricanu et al., 2003; Yang, Wang, Regenstein, & Rouse, 2007; Yang et al., 2008) but with different diameters. The significant difference in particle size, at different concentrations of gelatin, shows that the protonation or deprotonation of the amino or carboxylic acid residues in the gelatin molecules impacts the way the gelatin molecules fold together as particles form or there might be a difference in cross-linking among different concentrations (Saxena et al., 2005).

Table 1 shows the effects of concentrations on the physical properties of gelatin. The viscosity of gelatin increased with the concentrations. There was no statistical difference of the viscosity between the concentrations of 0.25% and 1.00%, while there was

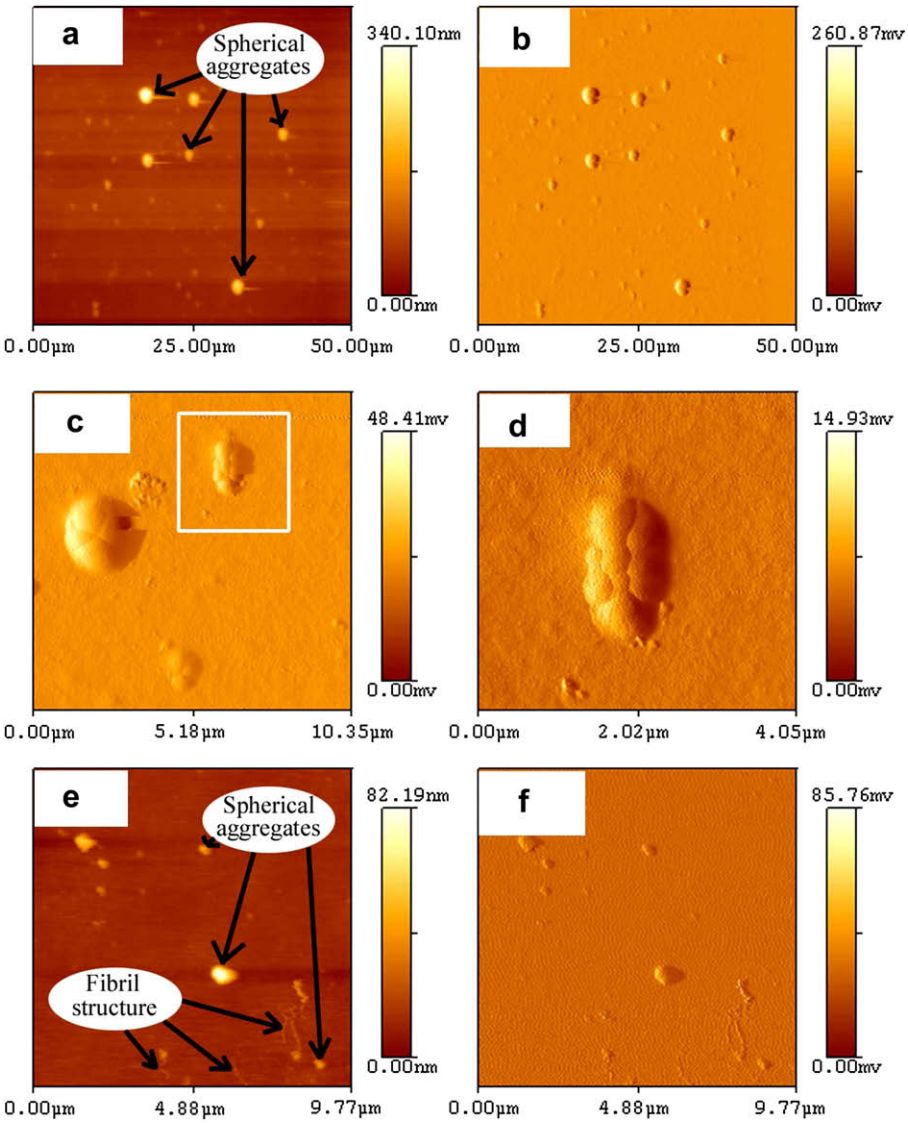

Fig. 4. AFM images of spherical aggregates and fibril structure in low concentration gelatin. (a) Plane image of 1% gelatin and (b) corresponding error-signal image of a; (c) another error-signal image of 1% gelatin and (d) enlarged image of c; (e) plane image of 0.25% gelatin and (f) corresponding error-signal image of e.

statistical difference between concentrations of 3.33% and 1%. There was also a large difference of TPA and gel strength between the concentrations above and below 1%, when the concentration was less than 1%, the gelatin could not form the gel well enough to allow determinations of TPA and gel strength, when the concentration was greater than 1%, the gel strength and some of the TPA parameters (hardness, chewiness) increased quickly with increase of concentration.

3.3. Relationships among concentration, nanostructure and physical property of gelatin

Gelatin gels have a complex behavior. They are not simple homogeneous materials, but heterogeneous structures with concentrations that are aging-time-dependent (Yang, Wang, Regenstein, & Rouse, 2007; Yang et al., 2008). AFM have accessed to a certain extent to the native state of the molecules to multistranded helices

Table 1
Effect of gelatin concentration on viscosity and textural property

Gelatin concentration (%)	*V*/cP	Gel strength/g	Hardness/g	Cohesiveness	Springiness	Chewiness/g
6.67	15.91 ± 0.56^{a}	213.5 ± 9.2^{a}	1976 ± 437^{a}	0.92 ± 0.02^{a}	0.77 ± 0.03^{a}	1378 ± 243^{a}
3.33	4.00 ± 0.02^{b}	59.8 ± 5.4^{b}	609 ± 122^{b}	0.94 ± 0.00^{a}	0.80 ± 0.01^{a}	459 ± 94^{b}
1.00	1.30 ± 0.01^{c}	18.4 ± 0.4^{c}	493 ± 50^{b}	0.25 ± 0.05^{b}	0.63 ± 0.26^{a}	83 ± 48^{b}
0.50	1.00 ± 0.01^{cd}	–	–	–	–	–
0.25	0.79 ± 0.01^{cd}	–	–	–	–	–
0.10	0.63 ± 0.01^{d}	–	–	–	–	–
0.05	0.61 ± 0.01^{d}	–	–	–	–	–

Note: the character of '–' means the gel strength was not determined because the gelatin cannot form gel in that group. Values in the same column with different superscript letters indicate significant differences by the Duncan's multiple range test ($P < 0.05$).

and supramolecular assemblies (Uricanu et al., 2003). However, to date, for gelatin gels, there is no systematic study to link the physical properties, which are measured at the macroscale by classical bulk experiments, with data obtained by AFM (Uricanu et al., 2003).

Our results clearly revealed that when the gel concentration was greater than 1%, the gelatin nanostructure showed fibril structure, and the physical properties including textural properties and viscosity increased quickly with increase of concentration. While the concentration was lower than 1%, the nanostructures showed mainly spherical aggregates, and there were no large difference in textural properties and viscosity in a wide concentration range (0.05–1%). It indicates that high texture and viscosity values corresponded to fibril nanostructure of gelatin, and lower values of these physical properties corresponded to spherical aggregates.

Differences in nanostructure and physical property of gelatins with different concentrations were probably attributed to the following mechanisms. The gelatin molecules have both positively and negatively charged segments at all pHs. The two charged segments join together through electrostatic attraction if and only if they are within a distance. The nanoparticles of the gelatin are formed largely through inter- and intramolecular electrostatic interactions. In the first stage of nanoparticle formation, there is competition between intramolecular folding and intermolecular aggregate formation and they give rise to a poly-dispersed solution of gelatin nanoparticles (Saxena et al., 2005). The number density and size of these junction zones determine the gel properties (Mackie et al., 1998). The high concentrations of gelatin may have large number density and size of the junction zones resulting in large values of texture and viscosity in our experiments. Comparing between physical properties (texture and viscosity) and nanostructural results from AFM images, some information obtained from the two methods is overlapping while the other is complementary. Physical properties from a texture analyzer or Cannon–Fenske viscometer reveal the viscosity and textural properties of gelatin by whole sample-based and for well-defined deformation rates. But AFM results reveal highly local viscosity, elasticity or other textural properties near the interface of the material with a less well-defined deformation (Uricanu et al., 2003; Yang et al., 2008). Our results reveal that there existed close relationships among the concentration, nanostructure and physical property of gelatin. It also supports that AFM is an indispensable tool for analyzing and manipulating physical properties of gelatin at a nanoscale level.

4. Conclusions

The sample preparing methods for AFM imaging gelatin from fish skins with high concentration were explored and developed. Gelatins with high concentrations (1–6.67%) showed fibril nanostructure, which only occasionally appeared in gelatins with low concentrations (less than 1%). Gelatins with low concentrations mainly aggregated into spherical structure. Physical properties at a macroscale level (texture and viscosity) had a large transition at concentration of 1%. Changes of macroscale physical properties related to the transition of nanostructure at certain concentrations. It indicates that there exist close relationships among the concentration, nanostructure and physical property of gelatin.

Acknowledgements

This research project was financially supported by the Alabama Agricultural Experiment Station (AAES). Project 30600420 supported by National Natural Science Foundation of China also contributed to this research.

References

An, H., Yang, H., Liu, Z., & Zhang, Z. (2008). Effects of heating modes and sources on nanostructure of gelatinized starch molecules using atomic force microscopy. *LWT – Food Science and Technology, 41*, 1466–1471.

Badii, F., & Howell, N. K. (2006). Fish gelatin: structure, gelling properties and interaction with egg albumen proteins. *Food Hydrocolloids, 20*, 630–640.

Benmouna, F., & Johannsmann, D. (2004). Viscoelasticity of gelatin surfaces probed by AFM noise analysis. *Langmuir, 20*, 188–193.

Chen, X., Davies, M. C., Roberts, C. J., Tendler, S. J., Williams, P. M., Davies, J., et al. (1998). Interpretation of tapping mode atomic force microscopy data using amplitude-phase-distance measurements. *Ultramicroscopy, 75*, 171–181.

Djabourov, M., Bonnet, N., Kaplan, H., Favard, N., Favard, P., Lechaire, J. P., et al. (1993). 3D analysis of gelatin gel networks from transmission electron microscopy imaging. *Journal De Physique II, 3*, 611–624.

Foegeding, E. A. (2006). Food biophysics of protein gels: a challenge of nano and macroscopic proportions. *Food Biophysics, 1*, 41–50.

Gómez-Guillén, M. C., Turnay, J., Fernández-Díaz, M. D., Ulmo, N., Lizarbe, M. A., & Montero, P. (2002). Structural and physical properties of gelatin extracted from different marine species: a comparative study. *Food Hydrocolloids, 16*, 25–34.

Haugstad, G., & Gladfelter, W. L. (1993). Atomic force microscopy of AgBr crystals and adsorbed gelatin films. *Langmuir, 9*, 1594–1600.

Haugstad, G., & Gladfelter, W. L. (1994). Probing biopolymers with scanning force methods: adsorption, structure, properties, and transformation of gelatin on mica. *Langmuir, 10*, 4295–4306.

Jamilah, B., & Harvinder, K. G. (2002). Properties of gelatins from skins of fish – black tilapia (*Oreochromis mossambicus*) and red tilapia (*Oreochromis nilotica*). *Food Chemistry, 77*, 81–84.

Lin, W., Yan, Y., Mu, C., Li, W., Zhang, M., & Zhu, Q. (2002). Effect of pH on gelatin self-association investigated by laser light scattering and atomic force microscopy. *Polymer International, 51*, 233–238.

Mackie, A. R., Gunning, A. P., Ridout, M. J., & Morris, V. J. (1998). Gelation of gelatin observation in the bulk and at the air–water interface. *Biopolymers, 46*, 245–252.

Mohanty, B., & Bohidar, H. B. (2005). Microscopic structure of gelatin coacervates. *International Journal of Biological Macromolecules, 36*, 39–46.

NanoRule+™ 2.0 user's manual. (2004). Santa Clara. CA, USA: Pacific Nanotechnology, Inc.

Nordmark, T. S., & Ziegler, G. R. (2000). Quantitative assessment of phase composition and morphology of two-phase gelatin–pectin gels using fluroscence microscopy. *Food Hydrocolloids, 14*, 579–590.

Radmacher, M., Fritz, M., & Hansma, P. K. (1995). Imaging soft samples with the atomic force microscope: gelatin in water and propanol. *Biophysical Journal, 69*, 264–270.

Saxena, A., Sachin, K., Bohidar, H. B., & Verma, A. K. (2005). Effect of molecular weight heterogeneity on drug encapsulation efficiency of gelatin nano-particles. *Colloids and Surfaces B: Biointerfaces, 45*, 42–48.

Uricanu, V. I., Duits, M. H. G., Nelissen, R. M. F., Bennink, M. L., & Mellema, J. (2003). Local structure and elasticity of soft gelatin gels studied with atomic force microscopy. *Langmuir, 19*, 8182–8194.

Wainewright, F. W. (1977). Physical tests for gelatin and gelatin products. In A. G. Ward, & A. Courts (Eds.), *The science and technology of gelatin* (pp. 507–532). New York: Academic Press.

Wang, Y., Yang, H., & Regenstein, J. M. (2008). Characterization of fish gelatin at nanoscale using atomic force microscopy. *Food Biophysics, 3*, 269–272.

Yang, H., An, H., Feng, G., & Li, Y. (2005). Visualization and quantitative roughness analysis of peach skin by atomic force microscopy under storage. *LWT – Food Science and Technology, 38*, 571–577.

Yang, H., Lai, S., An, H., & Li, Y. (2006). Atomic force microscopy study of the ultrastructural changes of chelate-soluble pectin in peaches under controlled atmosphere storage. *Postharvest Biology and Technology, 39*, 75–83.

Yang, H., Wang, Y., Jiang, M., Oh, J. H., Herring, J., & Zhou, P. (2007). 2-Step optimization of the extraction and subsequent physical properties of channel catfish (*Ictalurus punctatus*) skin gelatin. *Journal of Food Science, 72*, C188–C195.

Yang, H., Wang, Y., Lai, S., An, H., Li, Y., & Chen, F. (2007). Application of atomic force microscopy as a nanotechnology tool in food science. *Journal of Food Science, 72*, R65–R75.

Yang, H., Wang, Y., Regenstein, J. M., & Rouse, D. B. (2007). Nanostructural characterization of catfish skin gelatin using atomic force microscopy. *Journal of Food Science, 72*, C430–C440.

Yang, H., Wang, Y., Zhou, P., & Regenstein, J. M. (2008). Effects of alkaline and acid pretreatment on the physical properties and nanostructures of the gelatin from channel catfish skins. *Food Hydrocolloids, 22*, 1541–1550.

Yao, K., Liu, W., Lin, Z., & Qiu, X. (1999). In situ atomic force microscopy measurement of the dynamic variation in the elastic modulus of swollen chitosan/gelatin hybrid polymer network gels in media of different pH. *Polymer International, 48*, 794–798.

Zhou, P., Mulvaney, S. J., & Regenstein, J. M. (2006). Properties of Alaska pollock skin gelatin: a comparison with tilapia and pork skin gelatins. *Journal of Food Science, 71*, C313–C321.